Kinetics and Mechanism of Formation of S-Nitrosocysteine

Sovathana Ly, Moshood K. Morakinyo and Reuben H. Simoyi*

Department of Chemistry, Portland State University, Portland, OR 97207-0751, USA.

ABSTRACT

The kinetics and mechanism of the nitrosation of cysteine by nitrous acid has been studied in acidic medium. The stoichiometry of the reaction is strictly 1:1, with the formation of one mole of S-nitrosocysteine (CySNO) from one mole of nitrous acid. Only two nitrosating agents were detected: nitrous acid itself and protonated nitrous acid which is the hydrated form of the nitrosonium cation, NO^+. Nitric oxide itself was not detected as a nitrosant. The bimolecular rate constant for the direct nitrosation of cysteine by nitrous acid was determined to be 6.4 ± 1.1 L mol^{-1} s^{-1}, while nitrosation by the nitrosonium cation has a rate constant of 6.8×10^3 L mol^{-1} s^{-1}. CySNO is short-lived, and decomposes completely to cystine and nitric oxide within 100 s in the presence of micromolar quantities of Cu(II) ions. Since the physiological environment contains many metal ions and metalloenzymes, it is unlikely that CySNO will be an effective carrier of NO.

1. Introduction

Perhaps the most remarkable aspect of nitric oxide is the lack of knowledge of its biological activity up until about 20 years ago. It was designated by *Science* magazine as the 'molecule of the year' in 1992 and by *Chemical and Engineering News* as 'superstar molecule' in 1993. And there is a good reason why it has received so much attention. Nitric oxide has been implicated in several important bioregulatory processes which include, among others, the control of blood pressure (vasodilation) and platelet aggregation.[1] It is a cytotoxic agent in the non-specific immune system,[2] a carcinogen,[3] and it also serves as a neurotransmitter in the brain and peripheral nervous system.[4] At a molar mass of only 30 g mol^{-1}, it is one of the smallest bioactive molecules known. Its chemistry has been intensively studied as a pollutant in combustion and in ionospheric chemistry. It is only recently that the focus is now on its reactivity in the physiological environment.

Very little is known about nitric oxide chemistry in the physiological environment, and the little that is known does not conform to expected behaviour of a supposedly radical species. For example, nitric oxide is not highly reactive as would be expected for a radical molecule and it does not readily dimerize. There is very little evidence in the literature that it reacts with more than a very small range of compounds. It is not as destructive biologically as the hydroxyl radical and superoxide anion radical, and thus its physiologically-observed cytotoxicity cannot be ascribed to its radical nature. Nitric oxide, however, is known to react with iron and some iron nitrosyls giving stable but not easily isolable products.[5–7] This reactivity allowed Furchgott to tie nitric oxide to the acetylcholine-induced endothelium-derived relaxation factor (EDRF) leading to perhaps the most widely studied physiological role of nitric oxide.[8–12] The proposed mechanism of vasodilation is through the activation of guanylate cyclase by interaction of NO[13–15] with the prosthetic Fe(II) ion and subsequent scission of the Fe(II)-histidine bond. The now known high affinity Fe-NO binding has been shown to activate guanylate cyclase to catalyze the conversion of guanyl triphosphate to cyclic guanyl monophosphate, leading to phosphorylation of the enzyme.[6,16–19]

The proposed mechanistic involvement of NO in vasodilation, which won Furchgott and co-workers the Nobel prize in chemistry had a serious flaw: the diffusivity and reactivity of NO. The aerobic environment afforded by the physiological medium indicates that NO would react with oxygen to form NO_2:
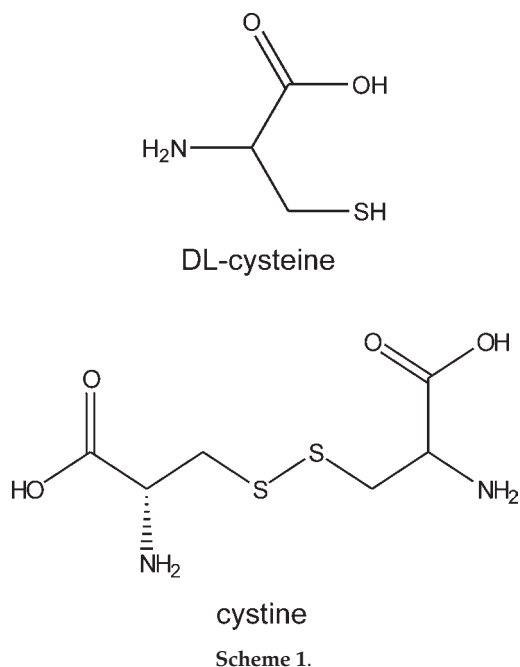
$$2NO + O_2 \rightarrow 2NO_2 \tag{1}$$

Equally, in the slightly basic physiological environment, NO would auto-oxidize[15] to NO_2^-. By calculating these reactivities and its spatial diffusivities, its lifetime would not be long enough to enable it to participate in all its postulated effects from its initial point of generation.[20] In the physiological environment, NO is synthesized via the oxidation of L-arginine to citrulline by the enzyme NO synthase.[21] Thus the major area of research is the search for possible mechanisms of transporting NO from point of generation to the point where it is needed to effect its physiological effects.

NO is known to react readily with thiols to form thionitrites (nitrosothiols), and the general conjecture is that these S-nitrosothiols are the most likely carriers of NO.[22–24] S-nitrosation, though believed to be irreversible, is still the only known viable transport mechanism for NO. This is due to the fact that the physiological effects of NO and nitrosothiols are interchangeable. While initially EDRF was thought to be in the form of nitrosothiols, since NO is the precursor to nitrosothiols, the exact form of EDRF has become blurred. Subsequent experimental data showed that NO is EDRF. Hence, mechanistic deduction of the formation of S-nitrosothiols from thiols and NO would greatly enhance our understanding of the physiological effects of NO.

In this manuscript we report on the detailed kinetics and mechanism of formation of S-nitrosocysteine. Cysteine is a hydrophilic non-essential aminoacid which can be synthesized by humans from methionine (Scheme 1). Cysteine is implicated in antioxidant defence mechanism against damaging species by increasing levels of the most dominant antioxidant, glutathione. It is involved in protein synthesis and is the precursor to the important aminosulphonic acid, taurine. The highly reactive thiol group, which exists as the thiolate group under physiologi-

---

* To whom correspondence should be addressed. E-mail: rsimoyi@pdx.edu

DL-cysteine

cystine

Scheme 1.

Figure 1 UV/visible spectral scan of reactants: (a) 0.04 mol L^{-1} CySH, (b) 0.03 mol L^{-1} NaNO$_2$, (c) 0.04 mol L^{-1} CySH + 0.03 mol L^{-1} NaNO$_2$, (d) 0.03 mol L^{-1} NaNO$_2$ + 0.05 mol L^{-1} H$^+$, (e) 0.04 mol L^{-1} CySH + 0.03 mol L^{-1} NaNO$_2$ + 0.05 mol L^{-1} H$^+$ and (f) 0.004 mol L^{-1} CySH + 0.003 mol L^{-1} NaNO$_2$ + 0.005 mol L^{-1} H$^+$.

cal conditions, is an excellent scavenger of reactive, damaging species. While its nitrosation is facile,[25] there has not been, to date, an exhaustive kinetic study of its formation to the extent that this manuscript is going to present. The kinetics of its formation and decomposition will aid in evaluating whether it could be an effective carrier of NO by deducing, from the kinetics, its possible lifetime.

2. Experimental

2.1. Materials

Doubly-distilled and deionized water (Barnstead Sybron Corporation water purification unit, Boston, MA, USA) was used for the preparation of all reagent stock solutions. The following reagents were used without further purification: DL-cysteine, EDTA, deuterated hydrochloric acid (99.8 %) (Sigma-Aldrich, St Louis, MO, USA), sodium nitrite, sodium chloride and hydrochloric acid (Fisher, Pittsburgh, PA, USA); cupric chloride (GFS Chemicals, Powell, OH, USA). Inductively-coupled plasma mass spectrometry showed that our aqueous medium contained 0.43 ppb Pb^{2+} as the metal ion with the highest concentration. The highly disruptive Cu^{2+} ions with respect to thiol reaction kinetics were present in negligible concentrations of less than 0.1 ppb.

2.2. Methods

Reactions were carried out at a constant ionic strength of 1.0 mol L^{-1} (NaClO$_4$) and at a temperature of 25.0 ± 0.1 °C. Absorption measurements were performed on a Perkin-Elmer UV/visible spectrophotometer (Perkin-Elmer, Boston, MA, USA). The absorptivity of S-nitrosocysteine was determined by mixing excess hydrochloric acid and sodium nitrite with DL-cysteine in mildly acidic conditions. The absorptivity was then determined by assuming that all the cysteine was converted to the nitrosothiol. In this way, an absorptivity of 17.2 L mol^{-1} cm^{-1} was deduced for S-nitrosocysteine at 544 nm. This is close to values obtained by other research workers. CySNO has another peak with a higher absorptivity at 335 nm. This peak, however, overlapped with, and was in close proximity to the absorption peaks of HNO$_2$ and NO$_2^-$ (see Fig. 1). The 544 nm peak was isolated and could be related solely to absorption contribution from CySNO. The nitrosation reaction was sufficiently rapid
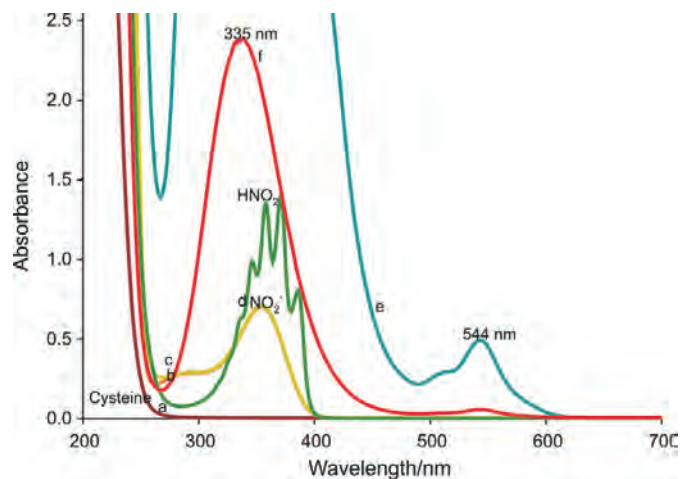
that accurate kinetic measurements were performed by following the formation of CySNO at 544 nm on a Hi-Tech Scientific SF61-DX2 stopped-flow spectrophotometer (Hi-Tech, Bradford-on-Avon, UK). The double mixing feature allowed for the initial formation of the nitrosating agent (HNO$_2$) which was then later reacted with cysteine after a suitable delay which could be varied to achieve the maximum nitrosation efficiency.

2.2.1. *The HPLC Technique*

The HPLC system utilized a Shimadzu (Columbia, MD, USA) SPD-M10A VP diode array detector, dual LC-600 pumps, LPT-6B LC-PC Interface controller, SIL-10AD auto injector, and Class-VP Chromatography Data System software. All samples were loaded on a reverse phase Discovery 5 μm C$_{18}$ HPLC column (Supelco, Bellefonte, PA, USA). They were run isocratically at 5 % acetonitrile/H$_2$O and all eluents were detected at a UV wavelength of 339 nm (for selective scans) with the maximum spectral scan mode employed to detect all eluents. A flow rate of 1 mL min^{-1} was maintained. All solutions for HPLC analysis were made using Milli-Q Millipore (Billerica, MA, USA) purified water and filtered using the Whatman (Florham Park, NJ, USA) Polypropylene 0.45 μm pore-size filter devices before injections (10 μL) into the column using the auto injector. To curb the interaction of the protonated amines on the analytes with the silanol groups on the stationary phase (which was causing tailing of the peaks) the sodium salt of 1-octanesulphonic acid (0.005 mol L^{-1}) was incorporated into the aqueous mobile phase. This was sufficient to neutralize the protonated amines and produce good resolution while eliminating peak tailing.

2.2.2. *Time of Flight Mass Spectrometry*

Mass spectra were acquired on a Micromass QTOF-II (Waters Corporation, Millford, MA, USA) quadrupole time-of-flight (QTOF) mass spectrometer. Analytes were dissolved in 50/50 acetonitrile/water, and analyte ions were generated by positive-mode electrospray ionization (ESI)[1] at a capillary voltage of 3.5 kV and a flow rate of 5 μL min^{-1}. The source block was maintained at 80 °C and the nitrogen desolvation gas was maintained at 150 °C and a flow rate of 400 L h^{-1}. Data were visualized and analyzed using the Micromass MassLynx 4.0 software suite for Windows 2000 (Waters Corporation, Millford, MA, USA).

O
‖
C
HO
S—N
O
NH₂
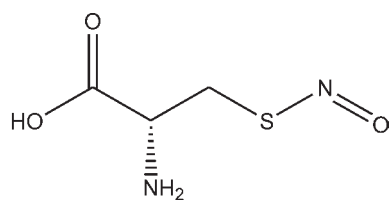
S-nitrosocysteine

Scheme 2.

3. Results

3.1. Stoichiometry

The stoichiometry of the reaction subscribed to other known nitrosation reactions in which one mole of NO reacts with one mole of the thiol to form the cysteine nitrosothiol with the elimination of a molecule of water.

S-Nitrosocysteine, CySNO (Scheme 2), was not as stable as the known secondary and tertiary nitrosothiols, but was stable at physiological and slightly basic environments for several minutes. The lifetime was sufficient to allow for the determina-

tion of the UV/visible spectrum (see Fig. 1, spectrum e). The spectrum shows that CySNO has an isolated absorption peak in the visible region at 544 nm. By running a series of experiments in equimolar excess nitrite and acid over cysteine, it was possible to evaluate the adopted absorptivity of 17.2 ± 0.1 L mol^{-1} cm^{-1} for CySNO at 544 nm. This was also confirmed by varying cysteine concentrations and testing the Beer-Lambert law on the basis of expected product formation. The other CySNO peak at 335 nm has a much higher absorptivity of 736 L mol^{-1} cm^{-1}, but at this wavelength, several other species in the reaction medium also absorb. Spectrum f was taken with very low cysteine concentrations in order to produce CySNO which would give an absorbance low enough at 335 nm to be measured on the absorbance scale in Fig. 1. All kinetic measurements were performed at 544 nm.

3.2. Product Determination

The relevant mass spectra for product determination are shown in Fig. 2. Within an hour of preparing the CySNO, the QTOF mass spectra gave a dominant peak at *m/z* 150.87 (see Fig. 2A) which would be the expected peak from CySNO from
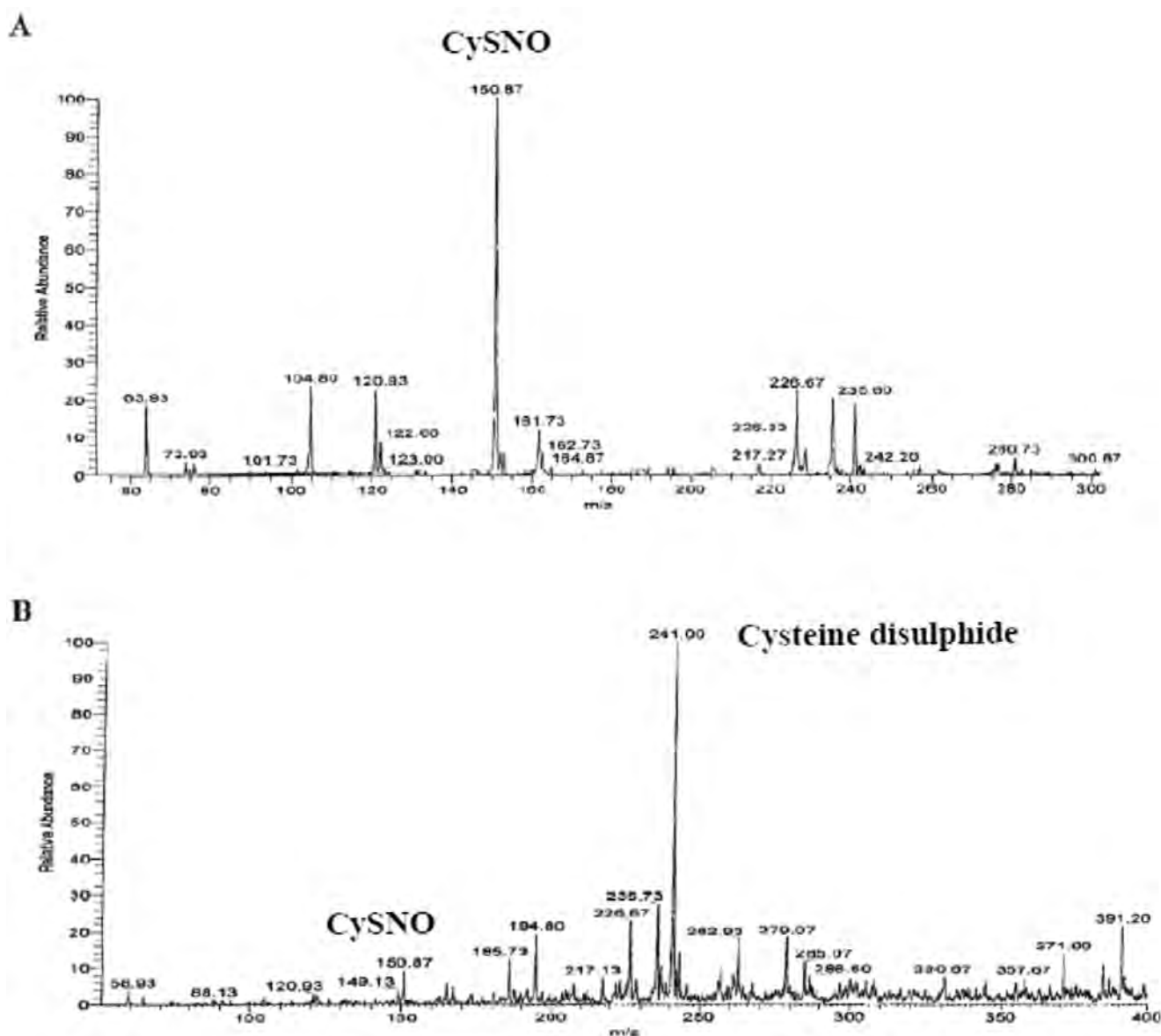

Figure 2 Mass spectrometry analysis of the product of nitrosation of CySH showing (**A**) formation of CySNO, m/z = 150.87, and (**B**) product of decomposition of CySNO after 24 h, cystine, a disulphide of CySH was produced with a strong peak at *m/z* = 241.00.
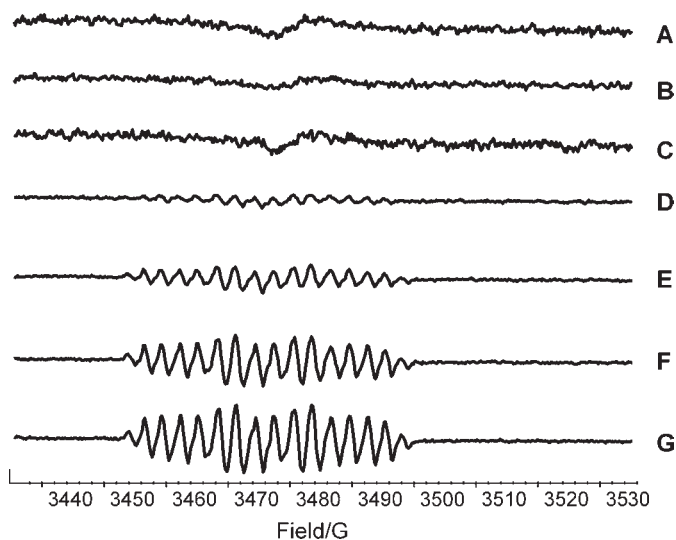
Figure 3 EPR spectra of NO radical generated during the decomposition of CySNO using 0.5 mol L^{-1} nitroethane (NE) in 1.0 mol L^{-1} NaOH solution as spin trap: (A) 0.5 mol L^{-1} NE, (B) 0.01 mol L^{-1} NO_2^-, (C) 0.04 mol L^{-1} CySH. [CySNO] = (D) 0.02 mol L^{-1}, (E) 0.03 mol L^{-1}, (F) 0.04 mol L^{-1} and (G) 0.05 mol L^{-1}.

the positive mode electrospray technique utilized. All other peaks observed in the spectrum are small and insignificant. Upon prolonged standing, the peak at m/z 150.87 slowly disappeared while being replaced by a peak at m/z 241.00, which is the expected peak for the cysteine disulphide, cystine (Scheme 1). Figure 2B is a spectrum of the products in Fig. 2A after 24 h. Over this period, the CySNO completely disappeared and the disulphide was nearly quantitatively formed. Several previous workers in this field had also concluded that the ultimate product in S-nitrosation is the oxidation of the thiol to the disulphide.[26–28]

$$2RSNO \rightarrow RSSR + 2NO \quad (2)$$

There has been some debate as to the veracity of reaction (2), with some schools of thought suggesting that the reaction may be strongly influenced by oxygen concentrations, or lack thereof. In alkaline solutions, nitroalkanes deprotonate to give an *aci*-anion, $RCH=NO_2^-$, which was recently discovered to be an excellent trap for NO, giving signature-type EPR spectra which can be used as evidence for the presence of NO.[29] Figure 3 shows a series of EPR spectra which prove the involvement of NO in CySNO decomposition. Pure trap, nitroethane, does not show any peaks without NO (spectrum A), while nitrite with the trap show no active peaks either (spectrum B), as does cysteine on its own (spectrum C). Spectra D–G show nitroethane with varying concentrations of CySNO. The peaks derived from the interaction of the trap with NO increase with concentrations of CySNO showing that the decomposition of CySNO involves release of NO.

$$2CySNO \rightarrow CySSCy + 2NO \quad (3)$$

3.3. Reaction Kinetics

Our study involved the simplest form of nitrosation: the one that involves the production of the nitrosating agent, HNO_2, in the same phase as the reactants and products. More complex forms of nitrosation involve the availing of gaseous nitric oxide through a nitric oxide-releasing compound. The biphasic nature of these nitrosations renders the subsequent kinetics and mechanisms complex. Through the use of the double-mixing feature of the stopped-flow ensemble, nitrous acid was initially formed by the mixing of hydrochloric acid and sodium nitrite and aged
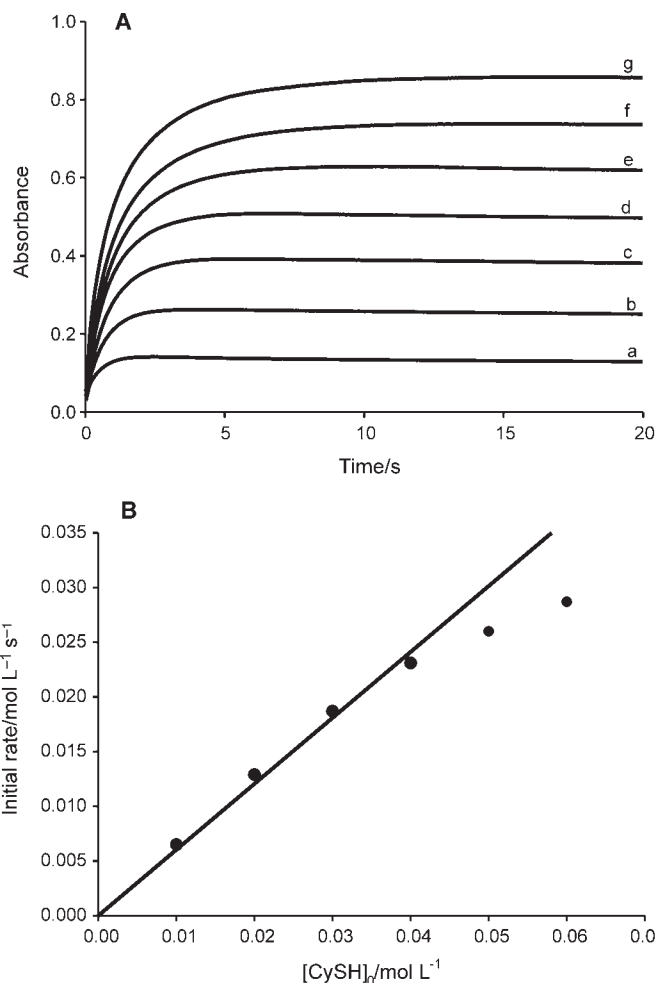

Figure 4 (A) Absorbance traces showing the effect of varying CySH concentrations. The reaction shows first-order kinetics in CySH. $[NO_2^-]_0 = 0.10$ mol L^{-1}; $[H^+]_0 = 0.10$ mol L^{-1}; $[CySH]_0 =$ (a) 0.01 mol L^{-1}, (b) 0.02 mol L^{-1}, (c) 0.03 mol L^{-1}, (d) 0.04 mol L^{-1}, (e) 0.05 mol L^{-1}, (f) 0.06 mol L^{-1} and (g) 0.07 mol L^{-1}. **(B)** Initial rate plot of the data in Fig. 4A. The plot shows strong dependence on initial rate of formation of CySNO on CySH.

for 1 s before being combined with the thiol in a third feed syringe to effect the nitrosation reaction. By assuming that protolytic reactions are fast, one can assume that the protonation of nitrite as well as other subsequent reactions would have reached equilibrium by the time the thiol was combined with the nitrosating agent. In general, the nitrosation kinetics were more reproducible when $[H^+]_0 \geq [NO_2^-]_0$. Reliable kinetic data used to evaluate rate constants utilized data in which acid concentrations were equal to or slightly greater than nitrite concentrations.

3.3.1. *Effect of Cysteine Concentrations*

For the evaluation of the effect of cysteine on the rate of reaction, equimolar concentrations of acid and nitrite were used. The final active concentrations of nitrite and acid at the beginning of the reaction were constant and could easily be evaluated from the acid dissociation constant of nitrous acid. Thus an increase in initial cysteine concentrations gave a linear and monotonic increase in cysteine concentrations in the reaction mixture without being affected by the nonlinear quadratic function that controls nitrite and acid concentrations. Figure 4A shows the absorbance traces obtained from a variation of initial
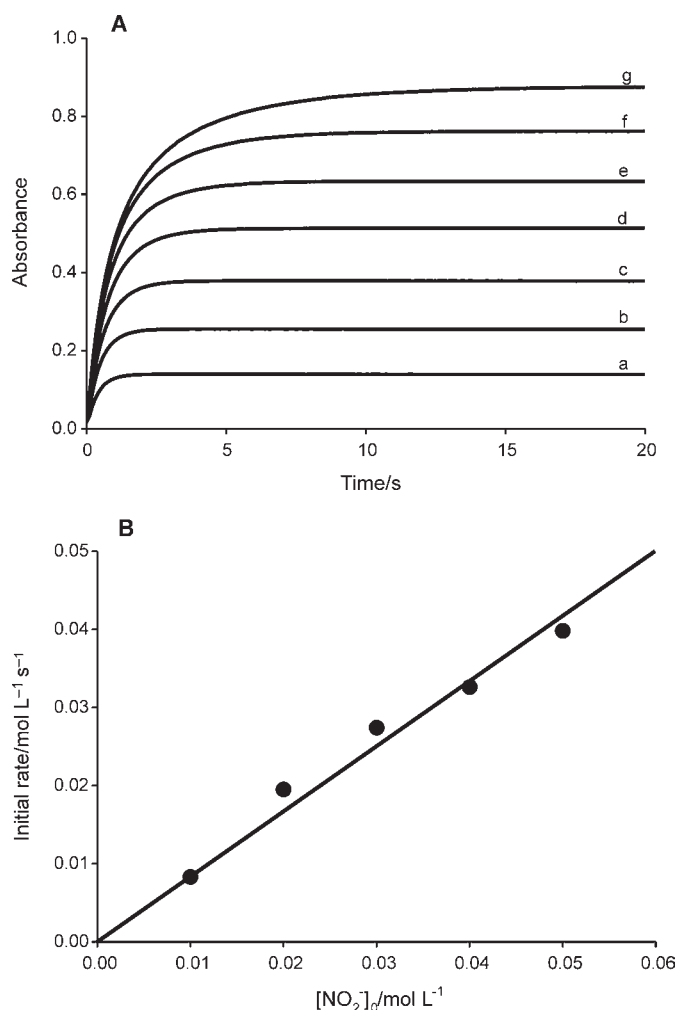
RESEARCH ARTICLE

S. Ly, M.K. Morakinyo and R.H. Simoyi,
S. Afr. J. Chem., 2010, **63**, 215–223,
<http://journals.sabinet.co.za/sajchem/>.

219

Figure 5 (A) Absorbance traces showing the effect of varying nitrite concentrations. The reaction shows first-order kinetics in nitrite. $[CySH]_0 = 0.10$ mol L^{-1}; $[H^+]_0 = 0.10$ mol L^{-1}; $[NO_2^-]_0 =$ (a) 0.01 mol L^{-1}, (b) 0.02 mol L^{-1}, (c) 0.03 mol L^{-1}, (d) 0.04 mol L^{-1}, (e) 0.05 mol L^{-1}, (f) 0.06 mol L^{-1} and (g) 0.07 mol L^{-1}. (**B**) Initial rate plot of the data in Fig. 5A. The plot shows strong dependence on the initial rate of formation of CySNO on nitrite.

cysteine concentrations. There was also a linear and monotonic increase in the final CySNO formed for as long as cysteine remained as the limiting reagent, which was the case for all the traces shown in Fig. 4A. Figure 4B shows that the effect of cysteine was linear, with a first order dependence. There was a noticeable saturation in the effect of cysteine on the initial rate of formation of CySNO at higher initial cysteine concentrations. Lower concentrations, however, gave a linear dependence with an intercept kinetically indistinguishable from zero as would have been expected in a system in which all cysteine is quantitatively converted to the nitrosothiol.

3.3.2. *Effect of Nitrite*

Figure 5A showed surprisingly simple and reproducible kinetics upon variation of nitrite. Data in Fig. 5A were derived from varying nitrite in regions where acid concentrations are in excess. A combination of data involving the variation of initial concentrations from below initial acid concentrations to above the acid concentrations did not retain linearity through the whole range of the plot because of the varying concentrations of HNO_2 formed that are nonlinearly dependent on the initial nitrite concentrations. With the conditions utilized for Figs. 5A and 5B; the changes in nitrosating agent, HNO_2, were clearly linearly

dependent on the initial nitrite concentrations. Thus the linear dependence on initial rate of formation of CySNO with nitrite concentrations shown in Fig. 5B was expected.

3.3.3. *Effect of Acid*

The effect of acid, as expected, was more complex (see Fig. 6A). The data in Fig. 6A involve changes in acid concentrations that spanned initial acid concentrations below nitrite concentrations to those in high excess over nitrite. The initial acid concentrations in Fig. 6A were increased stepwise by 1.00×10^{-2} mol L^{-1}; but the final acid concentrations in the reaction mixtures did not increase by the same constant rate due to the dissociation equilibrium of HNO_2. Thus a new table was created in which the final initial acid concentrations as well as nitrous acid and nitrite concentrations were calculated (see Table 1). These were the values utilized in the acid dependence plot shown in Fig. 6B. Available acid concentrations are heavily depressed in conditions under which the initial nitrite concentrations exceed the initial acid concentrations (first four data points in Fig. 6B). The next series of data points involves conditions in which the added acid concentrations exceeded those of nitrite. The resulting final free acid concentrations are derived from the excess acid plus the acid derived from the dissociation of nitrous acid. This dissociation is heavily depressed by the initial presence of excess acid, and thus there is a roughly linear relationship between the added acid and the final acid concentrations obtaining at the start of the reaction. Table 1 shows that when acid concentration exceeds nitrite concentrations ($[H^+]_0 > 0.05$ mol L^{-1}), the final acid concentrations are directly proportional to the initial added acid concentrations and that nitrous acid concentrations remain nearly constant in this range while asymptotically approaching 0.05 mol L^{-1}. Since initial nitrite concentrations were constant, the constant concentrations of HNO_2 in this range are expected and the effect of acid can thus be isolated. The linear plot observed for the effect of acid in this range suggests first order kinetics in acid for the nitrosation reaction (see Fig. 6C). It is also important to note that in the first four data points in Fig. 6B, there is a wild variation in both acid and the nitrosating agent, HNO_2 (see Table 1). The discontinuity in acid effect occurs when initial acid concentrations exceed initial nitrite concentrations, and final nitrite concentrations after acid equilibrium has been effected become negligible. Table 1 can be used to evaluate the effects of each of the relevant species in solution towards nitrosation. This is shown in Fig. 6D. In this figure, rate of nitrosation is plotted against nitrite, nitrous acid and acid concentrations. It shows that nitrite is not really involved in the nitrosation as the nitrosation rate is not reduced, even as nitrite concentrations become very small. Increase in nitrous acid concentrations, however, catalyzes nitrosation up to 0.05 mol L^{-1} (its maximum), but the fact that the rate of nitrosation keeps increasing despite static nitrous acid concentrations implies the presence of another nitrosant. Although the nitrosation rate is discontinuous in acid concentrations, there is, generally, a monotonic catalysis of nitrosation by acid.

3.3.4. *Effect of Cu^{2+} Ions*

The established experimental data implicate Cu^+ ions in the catalysis of decomposition of nitrosothiols. However, Fig. 7A shows that Cu(II) ions are extremely effective catalysts in the formation of CySNO when they are in the millimolar concentration range and even lower (data not shown). A plot to evaluate the effect of Cu(II) ions quantitatively is shown in Fig. 7B. It shows the typical catalyst effect that indicates an ever-increasing rate with Cu(II) followed by saturation. The
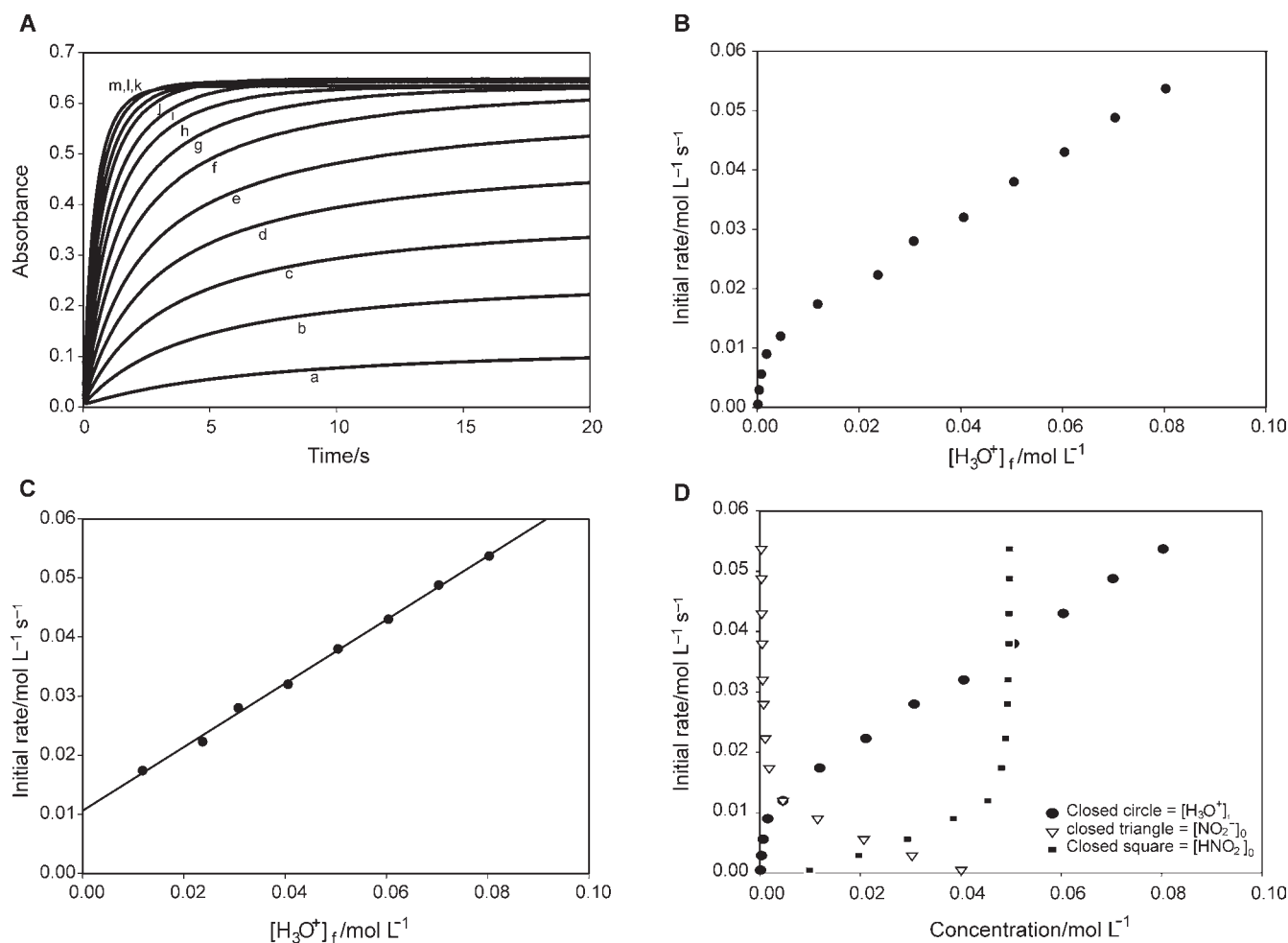
Figure 6 (**A**) Effect of low to high acid concentrations on the formation of CySNO. $[CySH]_0 = 0.05$ mol L^{-1}; $[NO_2^-]_0 = 0.05$ mol L^{-1}; $[H^+]_0 =$ (a) 0.01 mol L^{-1}, (b) 0.02 mol L^{-1}, (c) 0.04 mol L^{-1}, (d) 0.05 mol L^{-1}, (e) 0.06 mol L^{-1}, (f) 0.07 mol L^{-1}, (g) 0.08 mol L^{-1}, (h) 0.09 mol L^{-1}, (j) 0.10 mol L^{-1}, (k) 0.11 mol L^{-1}, (l) 0.12 mol L^{-1} and (m) 0.13 mol L^{-1}. (**B**) Initial rate plot of the data in Fig. 6A showing first-order dependence of the rate of formation of CySNO on acid at high acid concentrations. NO^+ is the main nitrosating agent. (**C**) Effect of acid on nitrosation in the high acid range. The intercept value should give an estimate of the nitrosation effect of nitrous acid without excess acid. (**D**) An evaluation of the effects of nitrite, nitrous acid and excess acid on the rate of nitrosation. Plot shows that nitrite is not involved in nitrosation, and that after the saturation of nitrous acid concentrations, a new nitrosant emerges, whose formation is catalyzed by acid.

micromolar Cu(II) concentration ranges are shown in Fig. 7C. Figure 7C also involves a longer observation time that encompasses both the formation and the consumption of CySNO. This figure shows that, even though Cu(II) ions catalyze the formation of CySNO, they also catalyze the decomposition of CySNO. Thus, in the presence of Cu(II) ions, the maximum expected quantitative formation of CySNO is not observed since the onset

of decomposition of CySNO is strongly enhanced in the presence of Cu(II) ions.

3.3.5. *Decomposition of CySNO*

The lifetime of CySNO in the physiological environment is determined by its rate of decomposition, especially at physiological pH conditions. Figure 8 shows the decomposition kinetics of

Table 1 Calculations of the final reactive species concentrations for acid dependence data shown in Figs. 6A and 6B.

$[H^+]_{added}$/mol L^{-1}	$[NO_2^-]_{added}$/mol L^{-1}	$[HNO_2]_0$/mol L^{-1}	$[NO_2^-]_0$/mol L^{-1}	$[H^+]_0$/mol L^{-1}
0.01	0.05	9.88×10^{-3}	4.01×10^{-2}	1.12×10^{-4}
0.02	0.05	1.97×10^{-2}	3.03×10^{-2}	2.99×10^{-4}
0.03	0.05	2.94×10^{-2}	2.07×10^{-2}	6.54×10^{-4}
0.04	0.05	3.85×10^{-2}	1.15×10^{-2}	1.53×10^{-3}
0.05	0.05	4.54×10^{-2}	4.59×10^{-3}	4.59×10^{-3}
0.06	0.05	4.81×10^{-2}	1.87×10^{-3}	1.19×10^{-2}
0.07	0.05	4.89×10^{-2}	1.07×10^{-3}	2.11×10^{-2}
0.08	0.05	4.93×10^{-2}	7.37×10^{-4}	3.07×10^{-2}
0.09	0.05	4.94×10^{-2}	5.60×10^{-4}	4.06×10^{-2}
0.10	0.05	4.96×10^{-2}	4.50×10^{-4}	5.05×10^{-2}
0.11	0.05	4.96×10^{-2}	3.80×10^{-4}	6.04×10^{-2}
0.12	0.05	4.97×10^{-2}	3.30×10^{-3}	7.03×10^{-2}
0.13	0.05	4.97×10^{-2}	2.90×10^{-3}	8.03×10^{-2}

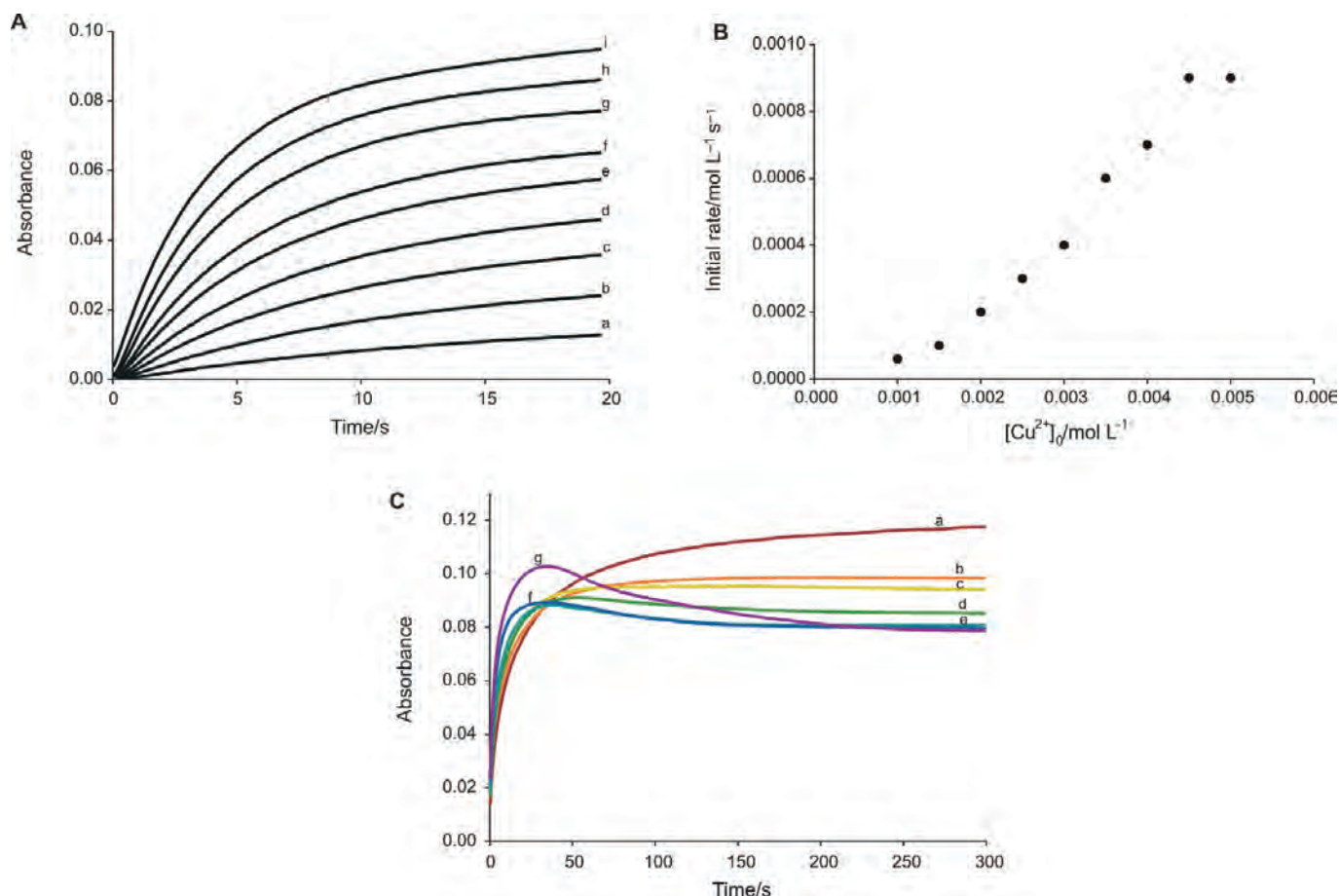**Figure 7** (**A**) Absorbance traces showing the effect of varying Cu^{2+} concentrations on the rate of formation of CySNO in the absence of perchloric acid. There is a progressive increase in the rate of CySNO formation with increase in Cu^{2+} concentration. $[CySH]_0 = [NO_2^-]_0 = 0.05$ mol L^{-1} ; $[H^+]_0 = 0.00$ mol L^{-1}; $[Cu^{2+}]_0 =$ (a) 0.001 mol L^{-1}, (b) 0.0015 mol L^{-1}, (c) 0.002 mol L^{-1}, (d) 0.0025 mol L^{-1}, (e) 0.003 mol L^{-1}, (f) 0.0035 mol L^{-1}, (g) 0.004 mol L^{-1}, (h) 0.0045 mol L^{-1} and (j) 0.005 mol L^{-1}. (**B**) Initial rate plot of the data in Fig. 7A showing the catalytic effect of copper. (**C**) Absorbance traces showing the effect of varying Cu^{2+} concentrations on the rate of formation of CySNO in the presence of perchloric acid. There is a progressive increase in the rate of CySNO formation with increase in Cu^{2+} concentration. High Cu^{2+} concentrations give an early onset of the decomposition of CySNO. $[CySH]_0 = [NO_2^-]_0 = [H^+]_0 = 0.01$ mol L^{-1}; $[Cu^{2+}]_0 =$ (a) 0.00 mol L^{-1}, (b) 1.0×10^{-6} mol L^{-1}, (c) 2.5×10^{-6} mol L^{-1}, (d) 5.0×10^{-6} mol L^{-1}, (e) 1.0×10^{-5} mol L^{-1}, (f) 5.0×10^{-5} mol L^{-1} and (g) 1.0×10^{-4} mol L^{-1}.

CySNO. Decomposition of nitrosothiols is metal ion-mediated. Trace a shows the slow decomposition of CySNO using normal reagent water and without chelators to sequester metal ions (mostly 0.43 ppb of Pb^{2+} according to our ICPMS analysis). Trace b shows the same solution as in trace a, but this time with EDTA added to sequester any metal ions. This shows that the decomposition of CySNO becomes even slower under these conditions; proving that even the very low metal ion concentrations present in reagent water are effective in catalyzing the decomposition of CySNO. The rest of the traces show ever-increasing concentrations of Cu^{2+} ions, but still in the micromolar range. There is noticeable autocatalysis in the rate of decomposition of CySNO.

4. Mechanism

Experimental data suggest a very simple nitrosation kinetics scheme that is first order in thiol and nitrite, with a slightly more complex dependence on acid. The acid effect has to be derived from its effect on the possible nitrosating agents. There are five possible nitrosating agents: HNO_2, N_2O_3, NO_2, NO and NO^+. Pure nitric oxide itself, NO, is highly unlikely to be a nitrosating agent in this environment, since the nitroethane spin trap did not trap any NO molecules during the formation of CySNO. Nitric oxide was observed only as a decomposition product (see Fig. 3). NO_2 and N_2O_3 are both derived from the autoxidation of nitric oxide:[30]

$$NO + \tfrac{1}{2}O_2 \rightarrow NO_2 \tag{4}$$

$$NO + NO_2 \rightarrow N_2O_3 \tag{5}$$

N_2O_3 and NO^+ are the strongest nitrosating agents out of

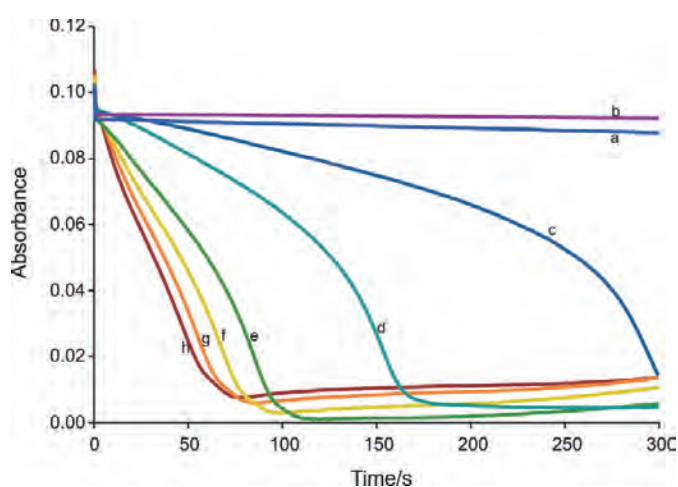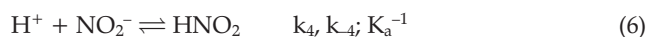**Figure 8** Effect of Cu^{2+} on the stability of CySNO in a pH 7.4 phosphate buffer. $[CySNO]_0 = 0.01$ mol L^{-1}; $[Cu^{2+}]_0 =$ (a) 0.00 mol L^{-1}, (b) 0.00 mol L^{-1} $Cu^{2+} + 1.0 \times 10^{-5}$ mol L^{-1} EDTA, (c) 5.0×10^{-6} mol L^{-1}, (d) 1.0×10^{-5} mol L^{-1}, (e) 2.0×10^{-5} mol L^{-1}, (f) 3.0×10^{-5} mol L^{-1}, (g) 4.0×10^{-5} mol L^{-1} and (h) 5.0×10^{-5} mol L^{-1}.

the five possibilities.[31] Formation of N_2O_3 is dependent on the dissolved oxygen in solution, which is normally at approximately 2.0×10^{-4} mol L^{-1}. NO concentrations are expected to be in the fractions of millimolar range. Thus both reactions (4) and (5) will not be effective in producing significant nitrosating agents. The elimination of three nitrosating agents leaves HNO_2 and NO^+, the nitrosonium cation,[32] as the predominant nitrosants. These two nitrosants both support first order kinetics in nitrite and thiol.

$$H^+ + NO_2^- \rightleftharpoons HNO_2 \qquad k_4, k_{-4}; K_a^{-1} \qquad (6)$$

$$HNO_2 + H^+ \rightleftharpoons NO^+ + H_2O \qquad k_5, k_{-5} \qquad (7)$$

$$CySH + HNO_2 \rightarrow CySNO + H_2O \qquad k_6 \qquad (8)$$

$$CySH + NO^+ \rightleftharpoons CySNO + H^+ \qquad k_7, k_{-7} \qquad (9)$$

Addition of reaction (7) is supported by the acid effect on the reaction which shows a strong acid dependence even when $[H^+]_0 > [NO_2^-]_0$. Without reaction (7), a quick saturation in acid effect should be observed when acid concentrations exceed nitrite concentrations since further increase in acid concentrations should leave the concentration of the single nitrosant, HNO_2, invariant. It is highly unlikely that the nitrosonium cation exists as the naked form in aqueous media, and one would expect it to be hydrated, HN^+OOH. Other groups represent it as protonated nitrous acid; H_2ONO^+. From the use of these two dominant nitrosants one can derive an initial rate of reaction:

$$
\begin{aligned}
\text{Rate} &= \frac{d[CySNO]}{dt} \\
&= \frac{[CySH][N(III)]_T[H^+]}{K_a + [H^+]}\left(k_6 + \frac{k_5 k_7[H^+]}{k_{-5}k_7[CySH]}\right)
\end{aligned}
\qquad (10)
$$

where

$$[N(III)]_T = [NO_2^-] + [HNO_2] + [RSNO] + [NO^+] \qquad (11)$$

Derivation of (10) from (11) was simplified by assuming that at the beginning of the reaction, concentrations of both the nitrosothiol and the nitrosonium ion are vanishingly small. Equation (10) can be further simplified by assuming that the forward and reverse rate constants for reaction (7) are rapid enough that the term $k_7[CySH]$ in the denominator can be discarded, giving:

$$\frac{d[RSNO]}{dt} = \frac{[CySH][N(III)]_T[H^+]}{K_a + [H^+]}(k_6 + K_5 k_7[H^+]) \qquad (12)$$

where K_5 is the equilibrium constant for the formation of the nitrosonium ion. Both Equations (10) and (12) are versatile enough to support all the observed kinetic behaviour of the system. This supports the observed first order kinetics in thiol and in nitrite concentrations (Figs. 4 and 5), and also supports the observed bifurcation in acid effects shown in Fig. 6B. These equations do not support second order kinetics, despite the possible dominance of reaction (7) in highly acidic environments, where the tandem of protonation of nitrite (6) and the further protonation of HNO_2 (7) would be a prerequisite for the formation of the nitrosant, culminating in second order kinetics. At low acid concentration, the second term in (10) (and in (11) as well) vanishes, and if low enough, where $K_a \gg [H_3O^+]$, first order kinetics would result. With such a low value of the nitrous acid dissociation constant, K_a, when acid is low, in the regions of $K_a \approx [H_3O^+]$, then acid behaviour would display the curving observed in the low acid concentration range of Fig. 6B. At high acid concentrations, where initial acid concentrations strongly exceed the dissociation constant of nitrous acid, the second term

will display first order kinetics while the first term will be kinetically silent with respect to acid. The first order dependence in acid observed in the high acid region of Fig. 6B confirms the mathematical form of Equation (11).
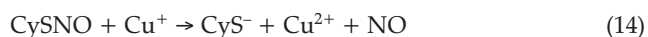
An evaluation of the bimolecular rate constant, k_6, can be made from the data shown in Figs. 4A and 4B. In this set of data, $[H^+]_0 = [NO_2^-]_0 = 0.10$ mol L^{-1} such that the final acid concentration at the beginning of the reaction is determined by the dissociation constant of 0.10 mol L^{-1} HNO_2. The millimolar concentrations of acid present nullify the second term in Equation (12), and the slope of the thiol dependence plot can be equated to $[N(III)]_T[H_3O^+]_0/(K_a + [H_3O^+]_0)$. These values will remain essentially constant for the range of the thiol concentrations used for this plot (Fig. 4B). Since the prevailing pH for these experiments is below the isoelectronic point of cysteine, it is reasonable to assume that a variation in thiol concentrations should not alter, significantly, the final acid concentrations. This evaluation gives $k_6 = 6.4 \pm 1.1$ L mol^{-1} s^{-1}.

The linear part of Fig. 6B can allow for the evaluation of the second bimolecular rate constant, k_7. Both the first and second terms in Equation (12) contribute to the overall rate of reaction, but any increase in rate with acid is solely on the basis of the second term since the first term saturates with respect to acid as the nitrous acid concentrations become invariant to further increases in acid. The intercept of Fig. 6B should enable the calculation of k_6. The value of the intercept was 1.06×10^{-2} L mol^{-1} s^{-1} and this was equated to $k_6[CySH]_0[N(III)]_T$ to yield $k_6 = 6.4$ L mol^{-1} s^{-1} (no error bars). This was exactly the same value as that derived from thiol dependence experiments shown in Fig. 4B. The congruence of these values for k_6, while derived from two separate approaches, proves the general veracity of this simple proposed mechanism. The slope can only enable the evaluation of $K_5 k_7$, and without an independent evaluation of k_7, it is not possible to evaluate an unambiguous value for k_6. From the rapid increase in nitrosation rate in response to acid increase after saturation of HNO_2, it appears that $k_7 > k_6$. The value of K_5 is heavily dependent on the pH and ionic strength of the reaction medium, and any value adopted for this study will be on the basis of how best this value can support the proposed equilibrium. By utilizing a previously-derived value of $K_5 = 3.162 \times 10^{-2}$ L mol^{-1}, Fig. 6B data evaluated $k_7 = 6.8 \times 10^3$ L mol^{-1} s^{-1} (no error bars could be calculated for this value).

4.1. Effect of Copper

Cu^+ is well known to be an efficient catalyst for nitrosothiol decomposition by preferentially binding to the S centre over the N centre of the nitrosothiol. This preferential binding, which in the model compound $HSN=O$ has been evaluated at 39.6 kJ mol^{-1} in favour of the S-binding, lengthens the S-N bond and facilitates its cleavage. Thus addition of Cu^+ ions to reactions involving the formation of nitrosothiols would show a progressive decrease in the yields of nitrosothiols with increasing additions of micromolar quantities of Cu^+ ions up to saturation. The interpretation of the effect of Cu^{2+} is a little more involved. Figures 7A and 7B clearly show that Cu^{2+} ions are catalytic in the formation of nitrosothiols. Figure 7B also shows the faintly sigmoidal increase in rate with increase in rate followed by a sharp saturation, which is a hallmark of most catalysis reaction dynamics. The general school of thought is that Cu^{2+} ions, in themselves, are innocuous in this environment, but that, in the presence of micromolar quantities of thiolate anions, redox-cycling would occur between Cu^{2+} and Cu^+, thereby effecting the catalysis.

$$2CyS^- + 2Cu^{2+} \rightarrow CySSCy \text{ (dimer)} + 2Cu^+ \qquad (13)$$

$$CySNO + Cu^+ \rightarrow CyS^- + Cu^{2+} + NO \qquad (14)$$

Data in Figs. 7A and 7B were obtained in the absence of acid to encourage the formation of the thiolate anions. Recent experimental data have shown that this effect of establishing redox cycling is not a preserve of thiolate anions exclusively, but any effective nucleophile in reaction medium such as ascorbate anions, halogens and pseudohalogens can bring about the sequence of reactions (13) and (14). In the absence of acid, Cu^{2+} catalyzes formation of the nitrosothiol, but on observing the long term effect of Cu^{2+} ions (Fig. 7C), one notices that even though Cu^{2+} ions catalyze the formation of the nitrosothiol, they also catalyze the decomposition of the nitrosothiol. Higher concentrations of copper ions rapidly form the nitrosothiol, and also encourage a rapid onset of decomposition.

Figure 8 attempts to simulate the physiological environment by using a phosphate buffer at pH 7.4. The nitrosocysteine was initially prepared and then combined with the various reagents shown in that figure to evaluate the decomposition kinetics of CySNO. The first two traces are displayed to show that there are negligible concentrations of metal ions in the distilled water utilized in our laboratories. The solution run with a metal ion sequester displays very similar kinetics to the one without EDTA. The ambient pH is above the isoelectronic point of cysteine, and thus will encourage formation of thiolate anions. The observed autocatalysis can be explained in a similar manner. Decomposition of CySNO will form the dimer, CySSCy, which can form more thiolate anions. Higher thiolate concentrations should increase the turnover number of the catalyst. Work by Stedman[33] showed the same autocatalysis in the decomposition and further reaction of formamidine disulphide with nitric oxide, which they explained through the formation of a pseudohalogen, SCN^-, which forms NOSCN.

5. Conclusion

The mechanism of nitrosation, though simple, differs with thiols and with reaction conditions, especially pH. In this manuscript, the two major nitrosants are nitrous acid itself and the nitrosonium ion, which is formed from the further protonation of the weak nitrous acid. There was no strong evidence to evoke the possibility of N_2O_3 as a contributing nitrosant. Its exclusion still gave a kinetic rate law that was strongly supported by the experimental data. Cysteine nitrosothiol does not seem to have a long enough half-life in the physiological environment to enable it to be an NO carrier. The general school of thought is that since the EDRF can be linked with NO, then the interaction of NO with protein thiol residues should be the process by which it expresses its physiological activity. The most abundant thiol in the physiological environment is glutathione, and maybe its nitrosothiol may be more robust in the human body, thus making it the most likely candidate for the transport of NO. This manuscript has proved that the nitrosothiol from cysteine is not that stable, decomposing completely in the presence of micromolar quantities of copper within 100 s. With the large numbers of metal ions and metalloenzymes in the physiological environment, one expects the lifetime of a cysteine nitrosothiol to be even shorter.

References

1 L.J. Marnett, *Chem. Res. Toxicol.,* 1996, **9**, 807–808.

2 H.K.F. Lau, *Atherosclerosis,* 2003, **166**, 223–232.

3 J.I. Murata, M. Tada, R.D. Iggo, Y. Sawamura, Y. Shinohe and H. Abe, *Mutat. Res. Fund. Mol. Mech. Mutagen.,* 1997, **379**, 211–218.

4 H.Y. Yun, V.L. Dawson and T.M. Dawson, *Mol. Psychiatry,* 1997, **2**, 300–310.

5 D.E. Coufal, P. Tavares, A.S. Pereira, B.H. Hyunh and S.J. Lippard, *Biochemistry,* 1999, **38**, 4504–4513.

6 D.E. Coufal and S.J. Lippard, *Abstracts of Papers of the American Chemical Society,* 1997, **213**, 399–INOR.

7 T.C. Harrop, Z.J. Tonzetich, E. Reisner and S.J. Lippard, *J. Amer. Chem. Soc.,* 2008, **130**, 15602–15610.

8 R.F. Furchgott, *Biosci. Rept.,* 1999, **19**, 235–251.

9 R.F. Furchgott, *Angew. Chem. Intern. Edit. Engl.,* 1999, **38**, 1870–1880.

10 R.F. Furchgott, *J. Amer. Med. Assoc.,* 1996, **276**, 1186–1188.

11 R.F. Furchgott, M.T. Khan and D. Jothianandan, *Federat. Proc.,* 1987, **46**, 385.

12 R.F. Furchgott, *J. Cardiovasc. Pharmacol.,* 1993, **22**, S1–S2.

13 D.J. Hawkins, B.O. Meyrick and J.J. Murray, *Biochim. Biophys. Acta,* 1988, **969**, 289–296.

14 S. Moncada, R.M. Palmer and E.A. Higgs, *Hypertension,* 1988, **12**, 365–372.

15 M.A. Ortega and A.A. Aleixandre, *Pharmacol. Res.,* 2000, **42**, 421–427.

16 H. Ishikawa, B.G. Yun, S. Takahashi, H. Hori, R.L. Matts, K. Ishimori and I. Morishima, *J. Amer. Chem. Soc.,* 2002, **124**, 13696–13697.

17 S. Kazerounian, G.M. Pitari, I. Ruiz-Stewart, S. Schulz and S.A. Waldman, *Biochemistry,* 2002, **41**, 3396–3404.

18 I.S. Severina, *Vorpr. Med. Khim.,* 2002, **48**, 4–30.

19 J.P. Stasch, P. Schmidt, C. Alonso-Alija, H. Apeler, K. Dembowsky, M. Haerter, M. Heil, T. Minuth, E. Perzborn, U. Pleiss, M. Schramm, W. Schroeder, H. Schroder, E. Stahl, W. Steinke and F. Wunder, *Brit. J. Pharmacol.,* 2002, **136**, 773–783.

20 J.M. Vanderkooi, W.W. Wright and M. Erecinska, *Biochim. Biophys. Acta,* 1994, **1207**, 249–254.

21 M.A. Marletta, *J. Biol. Chem.,* 1993, **268**, 12231–12234.

22 W.N. Kuo, J.M. Kocis, M.J. Robinson, J. Nibbs and R. Nayar, *Front. Biosci.,* 2003, **8**, a143–a147.

23 I. Chipinda and R.H. Simoyi, *J. Phys. Chem. B,* 2006, **110**, 5052–5061.

24 N. Hogg, *Free Radic. Biol. Med.,* 2000, **28**, 1478–1486.

25 D. Jourd'heuil, L. Gray and M.B. Grisham, *Biochem. Biophys. Res. Commun.,* 2000, **273**, 22–26.

26 M. Keshive, S. Singh, J.S. Wishnok, S.R. Tannenbaum and W.M. Deen, *Chem. Res. Toxicol.,* 1996, **9**, 988–993.

27 R.J. Singh, N. Hogg, J. Joseph and B. Kalyanaraman, *J. Biol. Chem.,* 1996, **271**, 18596–18603.

28 Y.L. Zhao, P.R. McCarren, K.N. Houk, B.Y. Choi and E.J. Toone, *J. Amer. Chem. Soc.,* 2005, **127**, 10917–10924.

29 K.J. Reszka, P. Bilski and C.F. Chignell, *Nitric Oxide,* 2004, **10**, 53–59.

30 B. Markwalder, P. Gozel and H. Vandenbergh, *J. Phys. Chem.,* 1993, **97**, 5260–5265.

31 D. Jourd'heuil, F.L. Jourd'heuil and M. Feelisch, *J. Biol. Chem.,* 2003, **278**, 15720–15726.

32 G. Depetris, A. Dimarzio and F. Grandinetti, *J. Phys. Chem.,* 1991, **95**, 9782–9787.

33 V. Francisco, L. Garcia-Rio, J.A. Moreira and G. Stedman, *New J. Chem.,* 2008, **32**, 2292–2298.